Chinese Physics

Quantum interference effects in a multi-driven transition $F_g = 3 \leftrightarrow F_e = 2$*

Dong Ya-Bin(董雅宾), Zhang Jun-Xiang(张俊香)[†],
Wang Hai-Hong(王海红), and Gao Jiang-Rui(郜江瑞)

State Key Laboratory of Quantum Optics and Quantum Optics Devices, Institute of Opto-Electronics,

Shanxi University, Taiyuan 030006, China

We have theoretically and experimentally studied the quantum coherence effects of a degenerate transition $F_g = 3 \leftrightarrow F_e = 2$ system interacting with a weak linearly polarized (with $\sigma_{\pm}$ components) probe light and a strong linearly polarized (with $\sigma_{\pm}$ components) coupling field. Due to the competition between the drive Rabi frequency and the Zeeman splitting, electromagnetically induced transparency (EIT) and electromagnetically induced absorption (EIA) are present at the different values of applied magnetic field in the case where the Zeeman splitting of excited state Δe is larger than the Zeeman splitting of ground state Δg (i.e. $\Delta e > \Delta g$).

Keywords: quantum coherence, degenerate two-level system, Zeeman splitting
PACC: 3260V, 4225B, 4250

1. Introduction

When a multi-level atom is driven by coherent light, atomic state related optical fields evolve quantum mechanically and the atomic coherence between these states occurs. This quantum coherence in an atomic system is responsible for a large number of important effects such as electromagnetically induced transparency (EIT),[1,2] coherent population trapping (CPT),[3] lasing without inversion (LWI),[4,5] and refractive index enhancement.[6] The motivation of such studies lies in a wide range of potential applications in a quantum information system: for example, storage of quantum information in a coherent medium,[7] quantum computation,[6] quantum logic gate,[8] quantum switch[9] and quantum interferometric optical lithography.[10] A substantial enhancement of the absorption of a probe laser can occur when the drive laser is applied to a quasi-degenerate two-level atomic system forming an N-type scheme.[11] Akulshin's group[12−15] extensively studied the effects in atomic Rb vapour both experimentally and theoretically. Goren et al[16] distinguished between two different kinds of EIA. One is due to the transfer of co-

herence (TOC) between the excited and ground states via spontaneous decay, and the other can occur when the collision transfer of population (TOP) from the ground state to a reservoir is greater than that from the excited state. Gu et al theoretically studied the transitions $F_e = 0 \leftrightarrow F_g = 1$, $F_e = 1 \leftrightarrow F_g = 0$ and $F_e = 1 \leftrightarrow F_g = 2$,[17−19] and concluded that EIT and EIA were obtained due to the competition between the driver Rabi frequency and the Zeeman splitting. Liu et al reported that the transitions from EIT to EIA in the Λ system of near degenerate levels was due to a spontaneously generated coherence, i.e. relative phase of the two applied fields.[20] The experimental showing of the transfer of EIT into EIA for the case of $F_e < F_g$ was given by Kim et al, recently.[21]

Most of these phenomena have been widely studied in typical Λ-type and V-type three-level or four-level atomic systems (simple models). The experimental demonstration of these phenomena was often carried out in atoms such as rubidium.[22−24] The theoretical analysis based on simple models indicates that these effects are based on the atomic coherence and the destructive quantum interference among different

transition pathways. However, the atomic coherence terms and the possible interference pathways increase quadratically with the total number of levels (including the Zeeman sublevels), which can easily exceed 10 in the energy schemes of real atoms. One may ask whether the main features predicted from simple models can hold for real atomic systems. Therefore, in our paper, we theoretically and experimentally study the quantum coherence effects resulting from the competition between the coupling field and the Zeeman splitting, when two independent linearly polarized coherent fields interact on the transition $F_g = 3 \leftrightarrow F_e = 2$ employed as a degenerate two-level system, which can be realized in the hyperfine transition between the states $6^2S_{1/2}(F = 3)$ and $6^2P_{3/2}(F = 2)$ of Cs. On the whole, the degenerate two-level atom system that the Gu group[19] and other groups have studied is the one in which the coupling field is the linearly polarized light interacting on the transition $M_{F_g} \leftrightarrow M_{F_e} = M_{F_g}$ and the probe field is another linearly polarized light which has left circular polarized and right circular polarized components interacting on the transition

$$M_{F_g} \leftrightarrow M_{F_e} = M_{F_g} \pm 1 \,.$$

In this paper, not only the probe field but also the coupling field is the linearly polarized light which include left circular polarized and right circular polarized components interacting on the transition $M_{F_g} \leftrightarrow M_{F_e} = M_{F_g} \pm 1$. So both the coupling field and the probe field interact on all sub-levels of ground states while the coupling field or the probe field does not interact on some sub-levels of ground states in the original patterns. It results in the population distribution on the sub-levels in our model being different from the original patterns. Therefore, the different phenomena will appear.

2. Optical Bloch equations

Let us consider the transition $F_g = 3 \leftrightarrow F_e = 2$ as shown in Fig.1, driven and probed by two linearly lights with frequencies ω_c and ω_p respectively, which co-propagate along the vector direction of static magnetic field.
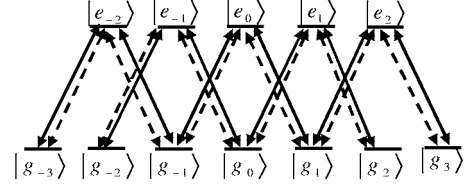

Fig.1. Zeeman sub-level structure for a transition $F_g = 3 \leftrightarrow F_e = 2$ and configuration of laser field. The coupling and probe fields are both coherent lights, which have circularly polarized components $\sigma_{\pm}$ each. Solid lines represent the coupling field, and dashed line is for the probe field.

According to the Zeeman effect, both fields have two equal left- and right-hand circularly polarized components $\sigma_{\pm}$ as long as the polarizations of two fields are orthogonal to the vector direction of static magnetic field, no matter the polarizations of two fields are orthogonal or parallel to each other. Here $\sigma_{\pm}$ lights interact with the transition $M_{F_e} = i \leftrightarrow M_{F_g} = i \pm 1$ with $i = 0, \pm 1, \pm 2$. The excited states are expressed as $|e_{-2}\rangle$, $|e_{-1}\rangle$, $|e_0\rangle$, $|e_1\rangle$ and $|e_2\rangle$, while the ground states are $|g_{-3}\rangle$, $|g_{-2}\rangle$, $|g_{-1}\rangle$, $|g_0\rangle$, $|g_1\rangle$, $|g_2\rangle$ and $|g_3\rangle$. Only the decays of the atomic levels due to spontaneous emission ($\Gamma_{eg} = \Gamma$) and collisions ($\Gamma_{ee} = \Gamma_{gg} = \Gamma_0$) that result in dephasing of the coherences and exchange of population between the Zeeman sublevels are considered.[17−19] In the rotating-wave approximation, the temporal evolution of the density matrix of the system is governed by

$$\dot{\rho}_{e_i g_j} = \frac{\mathrm{i}}{\hbar} \sum_k \left(V_{e_i g_k} \rho_{g_k g_j} - \rho_{e_i e_k} V_{e_k g_j} \right) - \left(\mathrm{i}\,\omega_{e_i g_j} + \gamma_{eg} \right) \rho_{e_i g_j} \,, \tag{1}$$

$$\dot{\rho}_{e_i e_i} = \frac{\mathrm{i}}{\hbar} \sum_k \left(V_{e_i g_k} \rho_{g_k e_i} - \rho_{e_i g_k} V_{g_k e_i} \right) - \left(7\Gamma + 4\Gamma_0 \right) \rho_{e_i e_i} + \Gamma_0 \sum_{j \neq i} \rho_{e_i e_j} \,, \tag{2}$$

$$\dot{\rho}_{e_i e_j} = \frac{\mathrm{i}}{\hbar} \sum_k \left(V_{e_i g_k} \rho_{g_k e_j} - \rho_{e_i g_k} V_{g_k e_j} \right) - \left(\mathrm{i}\,\omega_{e_i e_j} + \gamma_{ee} \right) \rho_{e_i e_j} \,, \tag{3}$$

$$\dot{\rho}_{g_i g_i} = \frac{\mathrm{i}}{\hbar} \sum_k \left(V_{g_i e_k} \rho_{e_k g_i} - \rho_{g_i e_k} V_{e_k g_i} \right) - 6\Gamma_0 \rho_{g_i g_i} + \Gamma \sum_{k=-2}^{2} \rho_{e_k e_k} + \Gamma_0 \sum_{j \neq i} \rho_{g_j g_j} \,, \tag{4}$$

$$\dot{\rho}_{g_i g_j} = \frac{\mathrm{i}}{\hbar} \sum_k \left(V_{g_i e_k} \rho_{e_k g_j} - \rho_{g_i e_k} V_{e_k g_j} \right) - \left(\mathrm{i}\,\omega_{g_i g_j} + \gamma_{gg} \right) \rho_{g_i g_j} \,, \tag{5}$$

where $V_{e_i g_j}$ represents the interacting energy for the $|e_i\rangle \rightarrow |g_j\rangle$ transition; $\omega_{e_i e_j} = \omega_{e_i} - \omega_{e_j}$ and $\omega_{g_i g_j} = \omega_{g_i} - \omega_{g_j}$ denote the Zeeman splittings of excited states and ground states respectively; $\omega_{k_i k_j} = g_k \mu_b B / \hbar$ $(i = j \pm 1)$ is the Raman detuning induced by the magnetic field with a strength of B, where g_k $(k = e$ or $g)$ is the Landé factor, μ_b is the Bohr magnetron; $\omega_{e_i g_j} = \omega_{e_i} - \omega_{g_j}$ is the transition frequency between excited and ground degenerate levels; $\gamma_{ee} = 7\Gamma + 4\Gamma_0$, $\gamma_{eg} = (7\Gamma + 10\Gamma_0)/2$, and $\gamma_{gg} = 6\Gamma_0$ are decay rates corresponding to different transitions. Ignoring the effect of spatial variation of the field amplitude, the interaction energy for the transition from the levels g_j to e_i is written as $V_{e_i g_j} = \hbar V_{e_i g_j}(\omega_c) e^{-i\omega_c t} + \hbar V_{e_i g_j}(\omega_p) e^{-i\omega_p t}$ with $i = 0, \pm 1, \pm 2, j = i \pm 1$. Here the magnitudes of $2V_{e_i g_j}(\omega_p) = \mu_{e_i g_j} E_p / 2^{1/2}\hbar$ and $2V_{e_i g_j}(\omega_c) = \mu_{e_i g_j} E_c / 2^{1/2}\hbar$ are the Rabi frequencies of probe and coupling fields respectively. The dipole moments of transitions are taken as $\mu_{e_{-2}g_{-3}} = \mu_{e_2 g_3} = -\sqrt{(5/14)}\mu$, $\mu_{e_{-2}g_{-1}} = \mu_{e_2 g_1} = -\sqrt{(1/42)}\mu$, $\mu_{e_{-1}g_{-2}} = \mu_{e_1 g_2} = -\sqrt{(5/21)}\mu$, $\mu_{e_{-1}g_0} = \mu_{e_1 g_0} = -\sqrt{(1/14)}\mu$ and $\mu_{e_0 g_{-1}} = \mu_{e_0 g_1} = -\sqrt{(1/7)}\mu$ for Cs D_2 line data.[25]

Considering the conditions under which the coupling light is much stronger than the probe light, we treat the coupling field to all orders in its Rabi frequency and meanwhile the probe field to the first order, then $\rho_{e_i g_j}$ oscillates at three frequencies:[26,27] the pump frequency ω_c, the probe frequency ω_p and the four-wave mixing frequency $2\omega_c - \omega_p$. We therefore express $\rho_{e_i g_j}$ in terms of its Fourier amplitudes as

$$\rho_{e_i g_j} = \rho_{e_i g_j}(\omega_c) e^{-i\omega_c t} + \rho_{e_i g_j}(\omega_p) e^{-i\omega_p t}$$
$$+ \rho_{e_i g_j}(2\omega_c - \omega_p) e^{-i(2\omega_c - \omega_p)t}. \quad (6)$$

Similarly, the populations and coherences within the same hyperfine level can be written as

$$\rho_{k_i k_j} = \rho_{k_i k_j}^{\mathrm{dc}} + \rho_{k_i k_j}(\omega_c - \omega_p) e^{-i(\omega_c - \omega_p)t}$$
$$+ \rho_{e_i g_j}(\omega_p - \omega_c) e^{-i(\omega_p - \omega_c)t}, \quad (7)$$

where $\rho_{k_i k_j}(\omega_c - \omega_p) e^{-i(\omega_c - \omega_p)t}$ and $\rho_{e_i g_j}(\omega_p - \omega_c) e^{-i(\omega_p - \omega_c)t}$ are population and coherence oscillations at frequencies $\omega_c - \omega_p$ and $\omega_p - \omega_c$ respectively. Since we are interested only in the steady-state results, we set the time derivatives of the Fourier amplitudes in Eqs.(1)–(5) equal zero. When the system is closed, it satisfies the relation: $\sum_i \rho_{e_i e_i} + \sum_j \rho_{e_j e_j} = 1$ with $i = 0, \pm 1, \pm 2$ and $j = 0, \pm 1, \pm 2, \pm 3$. And if the relation $\rho_{ij}(\omega_k) = \rho_{ij}^*(-\omega_k)$ is taken into account, these linear equations are readily solved.

The probe absorption is calculated from the imaginary part of the susceptibility $\chi(\omega_p)$. For transition $F_g = 3 \leftrightarrow F_e = 2$, we have

$$\chi(\omega_p) \propto [\mu_{e_{-2}g_{-3}}(\rho_{e_{-2}g_{-3}}(\omega_p) + \rho_{e_2 g_3}(\omega_p))$$
$$+ \mu_{e_{-2}g_{-1}}(\rho_{e_{-2}g_{-1}}(\omega_p) + \rho_{e_2 g_1}(\omega_p))$$
$$+ \mu_{e_{-1}g_{-2}}(\rho_{e_{-1}g_{-2}}(\omega_p) + \rho_{e_1 g_2}(\omega_p))$$
$$+ \mu_{e_{-1}g_0}(\rho_{e_{-1}g_0}(\omega_p) + \rho_{e_1 g_0}(\omega_p))$$
$$+ \mu_{e_0 g_{-1}}(\rho_{e_0 g_{-1}}(\omega_p)$$
$$+ \rho_{e_0 g_1}(\omega_p))]/(V_{e_0 g_{-1}}/\gamma_{eg}). \quad (8)$$

3. Quantum coherence effects

To model the quantum coherence effects of transition $F_g = 3 \leftrightarrow F_e = 2$ shown in Fig.1, we first define the parameters in the Bloch equations. If γ_{eg} is normalized to 1.0, then we have $\Gamma = 0.282$, $\Gamma_0 = 0.01\Gamma = 0.00282$, $\gamma_{ee} = 7\Gamma + 4\Gamma_0 = 1.983$ and $\gamma_{gg} = 6\Gamma_0 = 0.01692$. The frequency detuning of coupling light is $\Delta = \omega_c - \omega_{e_0 g_0}$, and the frequency detuning of probe is $\delta = \omega_p - \omega_{e_0 g_0}$. And we also let $V_{e_i g_j}(\omega_p)$ and $V_{e_i g_j}(\omega_c)$ be real for simplicity.

The absorption of the probe field as a function of frequency detuning of probe field is shown in Fig.2. In the case of no magnetic field applied, there is a typical EIT as shown in Fig.2(a). Here $V_c = E_c/2\sqrt{2}$ and $V_p = E_p/2\sqrt{2}$.

When a magnetic field is applied, the degeneracy is broken and Zeeman splitting is non-zero. In this case, not only the coherence between the Zeeman splitting and coupling field, but also the coherence among the Zeeman splittings belonging to different states, should be considered. Note that the Zeeman splitting Δe (or $\omega_{e_1 e_0}$) of the excited state is normally not equal to the splitting Δg (or $\omega_{g_1 g_0}$) of the ground state. Figures 2(b)–(d) show the quantum multi-coherence effects with the Zeeman splitting $\Delta e = 0.93B$, $\Delta g = 0.35B$ (here B is the intensity of magnetic field in CGS units), which corresponds to the actual Zeeman splitting of $6^2 S_{1/2}(F = 3)$ and $6^2 P_{3/2}(F = 2)$ states of Cs atoms.

As shown in Figs.2(a) and (b), when the intensity of magnetic field B is increased from $B = 0$ to $B = 0.4$ (Zeeman splitting is also increasing, but it is small compared with V_c), the spectrum changes from EIT to EIA. On further increasing the intensity of magnetic field B, the absorption peak becomes wider (see Fig.2(c)). If the intensity of magnetic field B becomes big compared with V_c as shown in Fig. 2(d), the

spectrum at resonance turns into transparency again; three transparency windows and two absorption peaks are observed in this case.
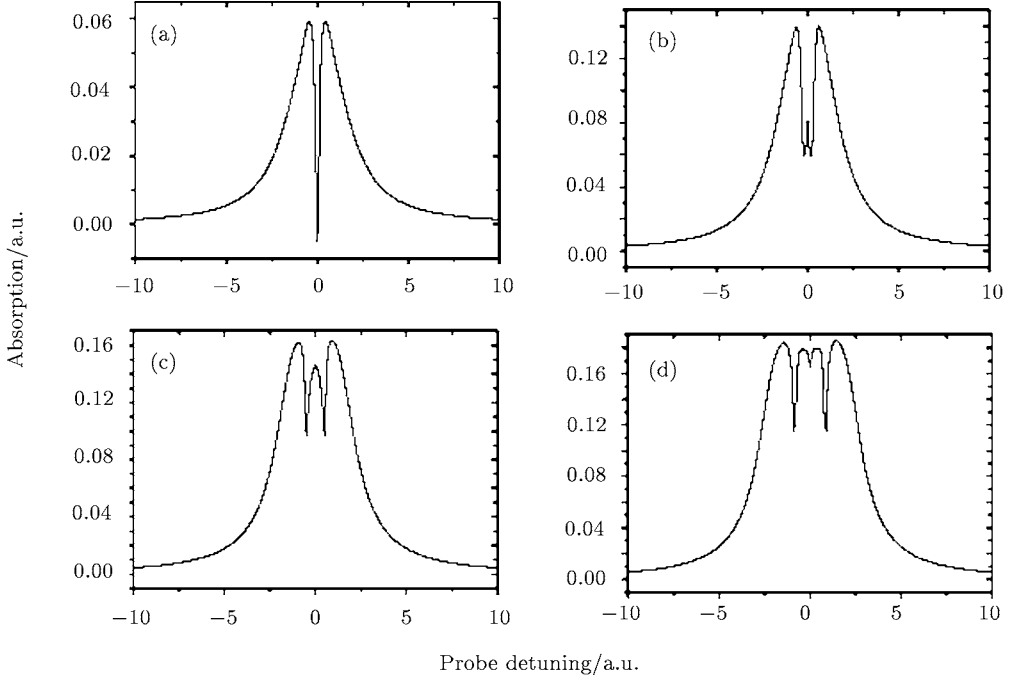

Fig.2.   The absorption of probe field as a function of frequency detuning of probe field at different Rabi frequencies of the coupling light with Zeeman splitting $\Delta e = 0.93B$ and $\Delta g = 0.35B$. (a) $B = 0$; (b) $B = 0.4$; (c) $B = 0.7$; (d) $B = 1.2$. Parameters are $V_c = 0.8$, $V_p = 0.8$, $\Gamma = 0.282$, $\Gamma_0 = 0.00282$, $\gamma_{ee} = 1.983$, $\gamma_{gg} = 0.01692$ and $\Delta = 0$.

4. Experimental setup and results

Figure 3 is the energy level configuration of the Cs D_2 line, the coupling and probe lights with frequencies ω_c and ω_p interact with the degenerate two-level system of $6S_{1/2}(F_g = 3) \leftrightarrow 6P_{3/2}(F_e = 2)$, which is closed because the transition from the excited level $6P_{3/2}(F_e = 2)$ to another ground level $6S_{1/2}(F_g = 4)$ is forbidden by the electric dipole selection rule.
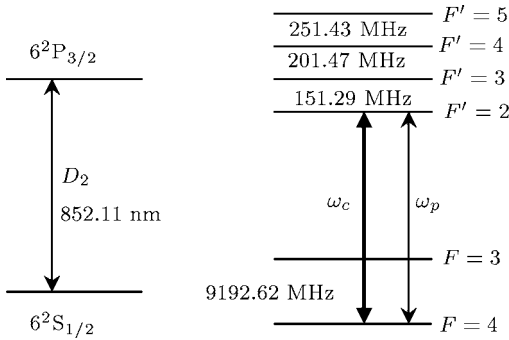

Fig.3.   Relevant energy diagram of the Cs D_2 line.

The experimental setup is shown in Fig.4. Two diode-lasers (TOPTICA; DL100) with less than 1MHz linewidth are used as coupling and probe laser lights respectively. The frequency of coupling beam is locked to the resonant transition between ground $F = 3(6S_{1/2})$ and excited $F' = 2(6P_{3/2})$ levels using the standard technology of saturation absorption spectrum with a lock-in amplifier and a proportional and integrating amplifier, while the frequency of the probe beam is scanned through the transition $6S_{1/2}(F_g = 3) \leftrightarrow 6P_{3/2}(F_e = 2)$. At the same time, the frequencies of two lasers are monitored by using Doppler free saturated absorption spectroscopy. Both the coupling and probe beams pass through an isolator to avoid the light feedback into the laser, then after half-wave plates, the two beams with linearly polarizations are overlapped on a polarizing beam prism before they enter the Cs vapour cell. The Cs cell is located in a spiral coil that can produce a longitudinal magnetic field (i.e. the quantization axis of magnetic field is perpendicular to the polarization of coupling and probe laser beams). And thus the two beams each can be treated as transverse lights with two equal left and right-hand circularly polarized components $\sigma_\pm$. After passing through the Cs cell, the probe and coupling beams are separated from each other by another

polarizing beam prism; the probe beam is detected by the photodiode and recorded by a digital oscilloscope. The spiral coil and the Cs vapour cell are shielded with μ metal sheets to prevent the magnetic field splitting of the sublevels from the surrounding magnetic field.
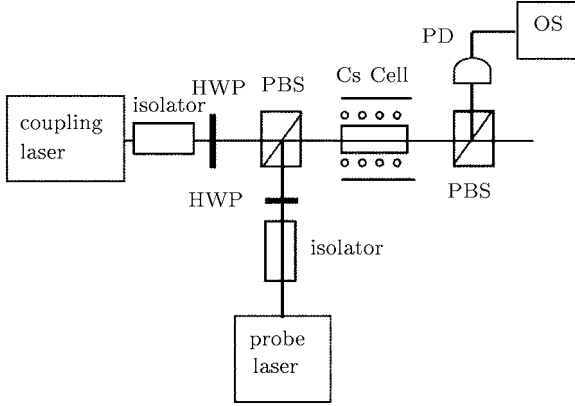

Fig.4. The experimental arrangement. PBS: polarizing beam splitter; PD: photo detector; HWP; half-wave plate; OS: oscilloscope.

When we lock the frequency of coupling laser to transition $6S_{1/2}(F_g = 3) \leftrightarrow 6P_{3/2}(F_e = 2)$, and meanwhile scan the frequency of probe laser across

$6S_{1/2}(F_g = 3) \leftrightarrow 6P_{3/2}(F_e = 2)$, the transmission spectra of probe laser are recorded as a function of probe detuning for different intensities of magnetic field B in Fig.5. The powers of coupling beam and probe beam are taken to be 2.21 mW and 0.21 mW respectively. As shown in Figs.5(a)–(d), the intensity of magnetic field B increases from 0 T to 1.2×10^{-3} T.

Figure 5(a) is the transmission spectrum when the magnetic field is turned off, as expected for quantum coherence in a two-level system, the signal of probe beam after the Cs cell exhibits the typical EIT effect. If the magnetic field is applied, the Zeeman splitting occurs, thus the degeneracies of both excited and ground levels are broken. In this case, the transmission spectra show the complex structure because of multi-coherence between the Zeeman splitting and coupling beam, and also the coherence among the Zeeman sublevels. We can see from the curve b in Fig.5 that the transparency peak is divided into two peaks. When the intensity of magnetic field B is continuously increased, the two EIT peaks are further separated (see Fig.5(c)). At last, a new transparency peak will appear in the centre of the curve as seen in Fig.5(d).
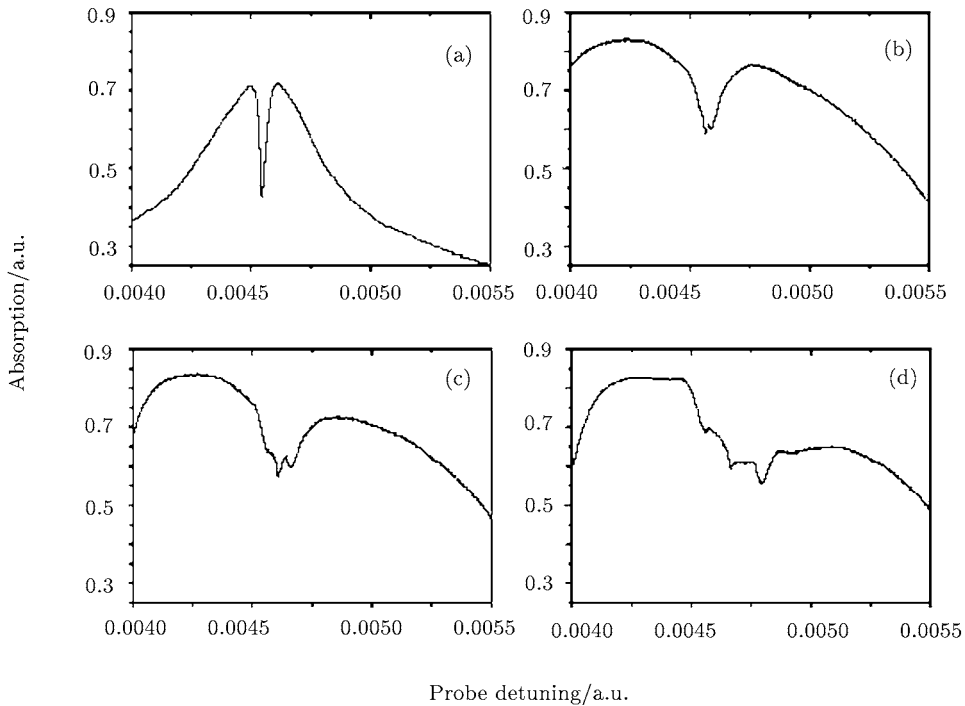

Fig.5. The transmission spectra as a function of prob detuning for different intensities of magnetic field B. Here, $P_c = 2.21$ mW and $P_p = 0.21$ mW. (a) EIT spectrum with the intensity of magnetic field $B = 0$ T. (b) and (c) the breaking up of the EIT peak with $B = 4 \times 10^{-4}$ T and $B = 7 \times 10^{-4}$ T. (d) The centre of spectra reverses again with $B = 1.2 \times 10^{-3}$ T.

It should be pointed out that all these quantum effects can be improved if the coupling and probe beams are phase locked. In this degenerate two-level system, it can be easily fulfilled by using one frequency stabilized laser beam and AOMs. One part of the beam, served as a coupling beam, is directly sent to Cs cell, and the other part of the beam, served as a probe beam, is sent to AOMs to be scanned across the transition before going through the Cs cell. In our experiment, it is limited by the laser power that we cannot use one laser to generate the coupling and probe beams, because the power of laser is attenuated a lot through AOMs. When this system is applied to accomplishing the multi-channel slow light transmission and storage of information, it may be important to use phase-locked laser beams to improve this effect, thus achieve the deep dispersion for slow light transmission.

The experimental results we have obtained in Fig.5 show that the two transparency peaks are not symmetrical in their heights and positions as we are supposed. It may come from the Doppler effects of atoms.

5. Conclusions

Quantum coherence effects of Zeeman hyperfine splitting in a two-level atomic system are studied when two independent linearly polarized coherent lasers interact on a degenerate two-level system, which is located in a static magnetic field. Both polarizations of coherent fields are orthogonal to the vector direction of the static magnetic field and they each have two equal left- and right-hand circularly polarized components $\sigma_\pm$ interacting with the transition $M_{F_e} = i \leftrightarrow M_{F_g} = i \pm 1$ with $i = 0, \pm 1, \pm 2$. If the intensity of magnetic field is zero, i.e. no Zeeman splitting, the atomic system is degenerate, only EIT can be found. If a magnetic field is applied along the light transmission direction, the degeneracy is broken, thus the multi-coherences are introduced, and both the EIT and EIA are obtained at the different intensities of magnetic field. And these effects are qualitatively consistent with the experimental results.

Acknowledgments

References

[1] Boller K J, Imamoğlu A and Harris S E 1991 *Phys. Rev. Lett.* **66** 2593

[2] Sun Q Q, Gu Y and Gong Q H, 2004 *Chin. Phys.* **13** 1716

[3] Gray H R, Whitley R M and Stroud C R, 1978 *Optics Lett.* **3** 218

[4] Harris S E 1989 *Phys. Rev. Lett.* **62** 1033

[5] Fan X J, Li P, Tian S F, Zhang J L and Liu Ch P 2001 *Chin. Phys.* **10** 613

[6] Scully M O, 1991 *Phys. Rev. Lett.* **67** 1855

[7] Phillips D F, Fleischhauer A, Mair A and Walsworth R L 2001 *Phys. Rev. Lett.* **86** 783

[8] Turchette Q A, Hood C J, Lange W, Mabuchi H and Kimble H J, 1995 *Phys. Rev. Lett.* **75** 4710

[9] Harris S E and Yamamoto Y 1998 *Phys. Rev. Lett.* **81** 3611

[10] Boto A N, Kok P, Abrams D S, Braunstein S L, Williams C P and Dowling J P 2000 *Phys. Rev. Lett.* **85** 2733

[11] Taichenachev A V, Tumaikin A M and Yudin V I 1999 *Phys. Rev. A* **61** 011802

[12] Akulshin A M, Barreiro S and Lezama A 1998 *Phys. Rev. A* **57** 2996

[13] Lezama A, Barreiro S and Akulshin A M 1999 *Phys. Rev. A* **59** 4732

[14] Lezama A, Barreiro S, Lipsich A and Akulshin A M 1999 *Phys. Rev. A* **61** 013801

[15] Lipsich A, Barreiro S, Akulshin A M and Lezama A 2000 *Phys. Rev. A* **61** 053803

[16] Goren C, Wilson-Gordon A D, Rosenbluh M and Friedmann H 2003 *Phys. Rev. A* **67** 033807

[17] Gu Y, Sun Q Q and Gong Q H 2003 *Phys. Rev. A* **67** 063809

[18] Sun Q Q, Gu Y and Gong Q Q, 2004 *J. Mod. Opt.* **51** 1899

[19] Gu Y, Sun Q Q and Gong Q H, 2004 *J. Phys. B* **37** 1553

[20] Liu Ch P, Gong Sh Q, Fan X J and Xu Z Z 2004 *Opt. Commun.* **231** 289

[21] Kim S K, Moon H S, Kim K and Kim J B 2003 *Phys. Rev. A* **68** 063813

[22] Xiao M, Li Y Q, Jin S and Gea-Banacloche J 1995 *Phys. Rev. Lett.* **74** 666

[23] Li Y Q and Xiao M 1995 *Phys. Rev. A* **51** R2703

[24] Moseley R R, Shepherd S, Fulton D J, Sinclair B D and Dunn M H, 1995 *Phys. Rev. Lett.* **74** 670

[25] Steck D A 2003 http://steck.us/alkalidata

[26] Wilson-Gordon A D and Friedmann H 1983 *Opt. Lett.* **8** 617

[27] Boyd Robert W, Raymer M G, Narum P and Harter D J 1981 *Phys. Rev. A* **24** 411